Acta Cryst E CRYSTALLOGRAPHIC COMMUNICATIONS

ISSN 2056-9890

Synthesis, crystal structure and Hirshfeld surface analysis of diaquabis(*o*-phenylenediamine-κ^2N,N')-nickel(II) naphthalene-1,5-disulfonate

Jabbor R Suyunov,[a] Khayit Kh. Turaev,[a] Bekmurod Kh. Alimnazarov,[a] Yusuf E. Nazarov,[a] Islombek J. Mengnorov,[b] Bakhtiyar T. Ibragimov[b] and Jamshid M. Ashurov[b]*

[a]Termez State University, "Barkamol avlod", at street, 43., Termez city, Uzbekistan, and [b]Institute of Bioorganic Chemistry, Academy of Sciences of Uzbekistan, 100125, M. Ulugbek Str 83, Tashkent, Uzbekistan. *Correspondence e-mail: ashurovjamshid1@gmail.com

Received 17 October 2023
Accepted 25 October 2023

Edited by M. Weil, Vienna University of Technology, Austria

Keywords: *o*-Phenylenediamine; 1,5-naphthalenedisulfonic acid; crystal structure; intermolecular interactions; hydrogen bonding; Hirshfeld surface.

CCDC reference: 2303464

Supporting information: this article has supporting information at journals.iucr.org/e

The reaction of *o*-phenylenediamine (OPD), sodium naphthalene1,5-disulfonate (Na_2NDS) and nickel sulfate in an ethanol–water mixture yielded the title compound, $[Ni(OPD)_2(H_2O)_2]\cdot NDS$ or $[Ni(C_6H_8N_2)_2(H_2O)_2](C_{10}H_6O_6S_2)$. This salt consists of a complex $[Ni(OPD)_2(H_2O)_2]^{2+}$ cation with two bidentate OPD ligands and *trans* aqua ligands, and a non-coordinating NDS^{2-} anion, which is the double-deprotonated form of H_2NDS. The Ni^{II} atom is situated at a center of inversion and exhibits a slightly tetragonally distorted $\{O_2N_4\}$ octahedral coordination environment, with four shorter equatorial Ni—N bonds [2.0775 (17) and 2.0924 (18) Å] and a longer axial Ni—O bond [2.1381 (17) Å]. The OPD ligand is located about an inversion center and is nearly coplanar with the NiN_4 plane [dihedral angle 0.95 (9)°]. In the crystal, the cations and anions are connected by charge-assisted intermolecular N—H···O and O—H···O hydrogen-bonding interactions into the tri-periodic network structure. Hirshfeld surface analysis indicates that the most important contributions to the crystal packing are from H···H (44.1%), O···H/H···O (34.3%), C···H/H···C (14.8%) C···C (6.5%) (involving the cations) and O···H/H···O (50%), H···H (25%), C···H/H···C (15.3%), C···C (8.2%) (involving the anions) interactions.

1. Chemical context

o-Phenylenediamine (OPD) condenses with ketones and aldehydes to a variety of useful products. Its reactions with carboxylic acids and their derivatives produce the important class of benzimidazoles (Vishvanath & Ketan, 2014; Aniket *et al.*, 2015; Pardeshi & Thore, 2015). Hence, OPD is commonly used in various industrial processes, including the production of dyes, polymers and the synthesis of fungicides, corrosion inhibitors, pigments, and pharmaceuticals (Abdullah *et al.*, 2019; Sagasser *et al.*, 2019; Pisarevskaya *et al.*, 2020; Jadoun *et al.*, 2021). It also exhibits electrical conductivity and is used in the production of conductive materials, such as sensors and batteries (Sayyah *et al.*, 2009; Bottari *et al.*, 2020). OPD is also a versatile ligand in coordination chemistry. It forms complexes with different metal ions, such as lanthanides (Koroteev *et al.*, 2020), zinc (González Guillen *et al.*, 2018; Zick & Geiger, 2016), cobalt (Ngopoh *et al.*, 2015; Konieczny *et al.*, 2019), copper (Djebli *et al.*, 2012; Chakraborty *et al.*, 2014), cadmium (González Guillen *et al.*, 2018) or nickel (Sabbani & Das, 2009; Lu *et al.*, 2009; Willett *et al.*, 2012; Adhikari *et al.*, 2021).

Compounds comprising 1,5-naphthalenedisulfonic acid (H_2NDS) or its deprotonated form (sulfonates) are of interest

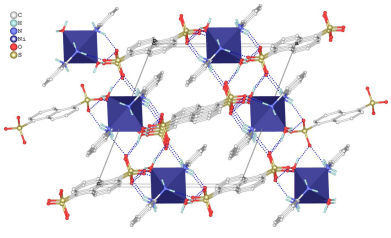

in supramolecular chemistry (Shi *et al.*, 2014; Xu *et al.*, 2019; Chen *et al.*, 2020), because the sulfonate group can accept up to six hydrogen bonds (Chen *et al.*, 2020; Oh *et al.*, 2020; Chen *et al.*, 2022). H_2NDS can react with organic compounds under formation of organic cations and the NDS^{2-} anion, or with metal compounds either under formation of non-coordinating NDS^{2-} anions, or with NDS^{2-} as a ligand (Huo *et al.*, 2005; Kokunov *et al.*, 2015). As a ligand, NDS^{2-} can bind in a bridging mode (Lian & Qu, 2013; Das *et al.*, 2015; Tai *et al.*, 2015).

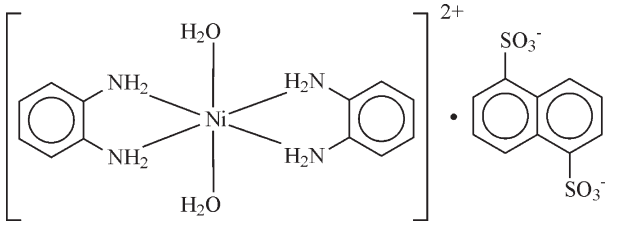

In this work, we focus on the synthesis, crystal structure, and Hirshfeld surface analysis of a nickel(II) complex, $[Ni(OPD)_2(H_2O)_2]\cdot NDS$, where the NDS^{2-} anion is not part of the metal coordination sphere.

2. Structural commentary

The structures of the molecular entities of the title compound are shown in Fig. 1. This salt consists of an Ni^{II}-centered complex cation with two bidentate OPD ligands and *trans*-aligned aqua ligands, as well as of a non-coordinating NDS^{2-} anion, which is the double-deprotonated form of H_2NDS. The Ni^{II} atom is situated at a crystallographic inversion center (Wyckoff letter *d* of space group $P2_1/n$) and exhibits a slightly tetragonally distorted $\{O_2N_4\}$ octahedral coordination environment, with two pairs of shorter equatorial Ni—N bonds [2.0775 (17) and 2.0924 (18) Å] and a pair of longer axial Ni—O bonds [2.1381 (17) Å]. The OPD ligand, likewise located over a crystallographic inversion center at the middle of the central C11—C11($-x+1, -y+2, -z+1$) bond, is almost coplanar with the NiN_4 plane, with a dihedral angle of 0.95 (9)°. The deviation of the ideal octahedral coordination sphere around nickel might be explained as follows: The inflexible nature of the OPDA ring system with an N···N distance between the amino groups of 2.770 (2) Å determines the N2—Ni1—N1 and N2—Ni1—N1($-x+2, -y+1, -z+1$) bite angles of 83.26 (7) and 96.74 (7) °, respectively.

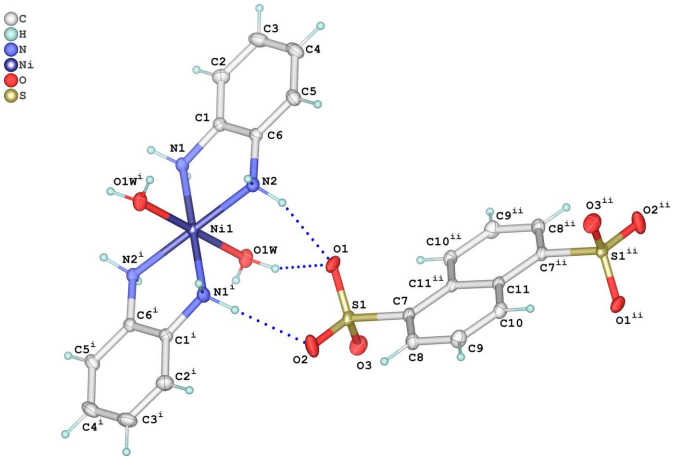

Figure 1
The structures of the molecular entities in the title salt, showing the atom-labeling scheme and displacement ellipsoids drawn at the 50% probability level. H atoms are shown as small spheres of arbitrary radius and hydrogen bonds are shown as dashed lines. [Symmetry codes: (i) $2-x, 1-y, 1-z$; (ii) $1-x, 2-y, 1-z$.]

Table 1
Hydrogen-bond geometry (Å, °).

D—H···A	D—H	H···A	D···A	D—H···A
N1—H1A···O2^{i}	0.89 (1)	2.48 (2)	3.268 (3)	148 (3)
N1—H1B···O2^{ii}	0.89 (1)	2.18 (1)	3.066 (3)	175 (3)
N2—H2A···O1	0.88 (1)	2.10 (1)	2.941 (2)	160 (3)
N2—H2B···O3^{iii}	0.89 (1)	2.06 (1)	2.908 (3)	158 (2)
O1W—H1WA···O3^{iv}	0.85 (1)	2.12 (2)	2.876 (3)	148 (3)
O1W—H1WB···O1	0.85 (1)	2.04 (2)	2.803 (2)	150 (3)

Symmetry codes: (i) $x, y-1, z$; (ii) $-x+2, -y+1, -z+1$; (iii) $x+\frac{1}{2}, -y+\frac{3}{2}, z+\frac{1}{2}$; (iv) $-x+\frac{3}{2}, y-\frac{1}{2}, -z+\frac{1}{2}$.

3. Supramolecular features and Hirshfeld surface analysis

In the crystal, the complex $Ni(OPD)_2(H_2O)_2]^{2+}$ cation and the NDS^{2-} anion are associated *via* charge-assisted intermolecular O—H···O and N—H···O hydrogen bonds (Table 1). Each $[Ni(OPD)_2(H_2O)_2]^{2+}$ cation forms N—H···O and O—H···O hydrogen bonds with six neighboring organic anions whereby the two aqua and two OPD ligands act solely as hydrogen-bonding donor groups (Fig. 2). All six acceptor oxygen atoms of the SO_3^- groups of the NDS^{2-} anions participate as double acceptor atoms (Fig. 3). Hydrogen bonds N1—H1B···O2^{iii}, N2—H2A···O1 and O1W–H1WB···O1 lead to the formation of supramolecular zigzag chains parallel to [100]. These chains are further connected by N1—H1A···O2^{ii} and N1—H1B···O2^{iii} hydrogen bonds, resulting in sheets parallel to (110). Additionally, cations and neighboring dianions are linked through O1W—H1WA···O3^{iv} and N2—H2B···O3^{i}

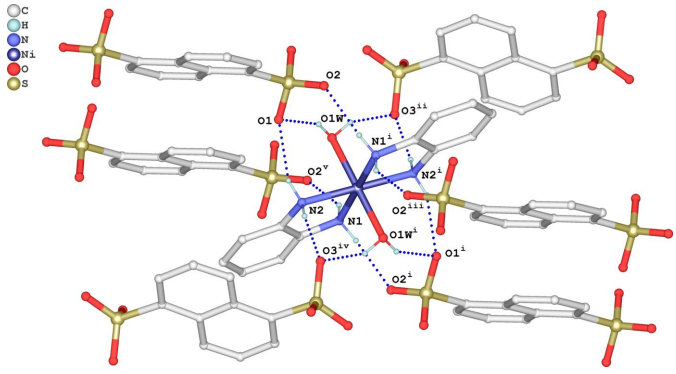

Figure 2
Formation of hydrogen bonds (dashed lines) between the $[Ni(OPD)_2(H_2O)_2]^{2+}$ cation with six neighboring anions. Symmetry codes refer to Table 1.

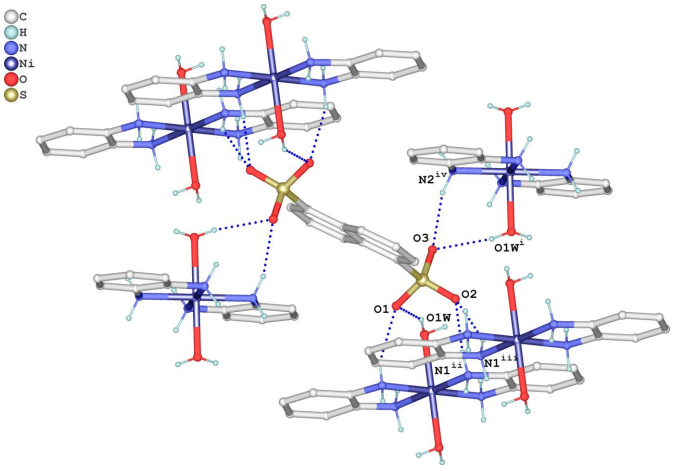

Figure 3
Formation of hydrogen bonds (dashed lines) between the NDS^{2-} anion with six neighboring cations. Symmetry codes refer to Table 1.

hydrogen bonds. The molecules stack along [001], thereby forming a consolidated tri-periodic supramolecular network (Fig. 4).

The supramolecular interactions discussed above were quantitatively investigated and visualized using Hirshfeld surface analysis performed with *CrystalExplorer* (Spackman *et al.*, 2021), with a standard resolution of the three-dimensional d_{norm} surfaces plotted over a fixed color scale of −0.5408 (red) to 1.4249 (blue) a.u.. Visualizations were performed using a red–white–blue color scheme, where red highlights contacts shorter than the sum of the van der Waals (vdW) radii, white contacts around vdW separations, and blue contacts longer than the sum of the vdW radii. It should be noted that the Hirshfeld surfaces and fingerprint plots were calculated separately for the $[Ni(OPD)_2(H_2O)_2]^{2+}$ cation and the NDS^{2-} dianion. The d_{norm} surface has twelve bright-red spots on the Hirshfeld surface for the cation and anion each (Fig. 5), resulting from the two O—H···O and four N—H···O intermolecular hydrogen bonds, as discussed above (Fig. 5; the number is doubled due to inversion symmetry for both enti-

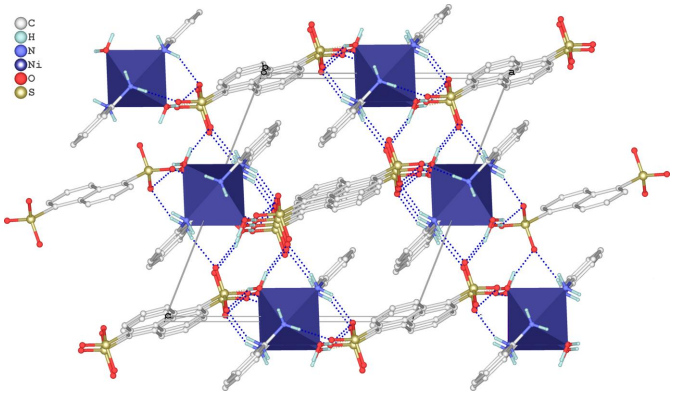

Figure 4
The crystal packing of the title salt in a view along [010] based on the formation of O—H···O and N—H···O hydrogen bonds (dashed blue lines). The coordination sphere around Ni^{II} is given in the polyhedral representation.

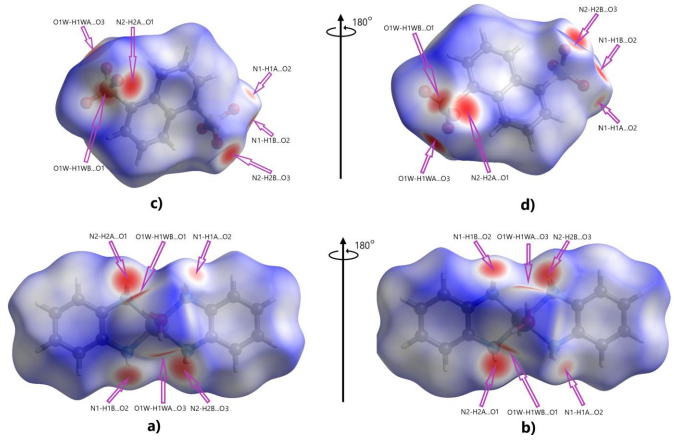

Figure 5
View of the three-dimensional Hirshfeld surface for the $[Ni(OPD)_2(H_2O)_2]^{2+}$ cation and the NDS^{2-} dianion plotted over d_{norm}. Parts (*a*) and (*b*) show the front and back sides, respectively, of the $[Ni(OPD)_2(H_2O)_2]^{2+}$ dication. Parts (*c*) and (*d*) show the front and back sides, respectively, of the NDS^{2-} dianion.

ties). The classical O—H···O and N—H···O hydrogen bonds correspond to H···H and H···O contacts in the two-dimensional fingerprint plots (with contributions of 44.1 and 50% to the Hirshfeld surface for the $[Ni(OPD)_2(H_2O)_2]^{2+}$ cation and NDS^{2-} anion, respectively; Fig. 6*b* and 6*f*). O···H/H···O and C···H/H···C, interactions in the cation, and H···H and C···H/H···C interactions in the dianion follow with contributions of 34.3, 14.8, 25 and 15.3%, respectively (Fig. 6*c*,*d*,*g*,*h*). Other minor contributions are from C···C (6.5%) and C···O (0.3%) contacts in the cation, and from C···C (8.2%), C···O (0.3%), O···O (0.1%) and S···H (0.1%) contacts in the dianion. The O···H/H···O contacts are visible as a spike with a sharp tip on the side of the corresponding two-dimensional fingerprint plot, which is indicative of strong intermolecular interactions between atoms. On the other hand, the C···H/H···C contacts form less pronounced spikes, suggesting that these interactions are much weaker.

4. Database survey

In a search of the Cambridge Structural Database (CSD, version 2022.3.0; Groom *et al.*, 2016), a total of 207 compounds containing the *o*-phenylenediamine moiety were identified. Out of these, 129 compounds were metal complexes, while 78 compounds were organic salts. One organic salt comprising protonated *o*-phenylenediamine and 1,5-naphthalenedisulfonate has been studied (CSD refcode PEFYOQ; Deng *et al.*, 2012). When searching with 1,5-naphthalenedisulfonic acid as the search criterion, 90 metal complexes and 170 organic salt compounds were found. In the majority of metal complexes, 1,5-naphthalenedisulfonic acid was found in its dianionic form and was not part of the coordination sphere. However, in ten cases a bridging mode for the 1,5-naphthalenedisulfonate anion was found. Only one compound was identified where the 1,5-naphthalenedisulfonate anion

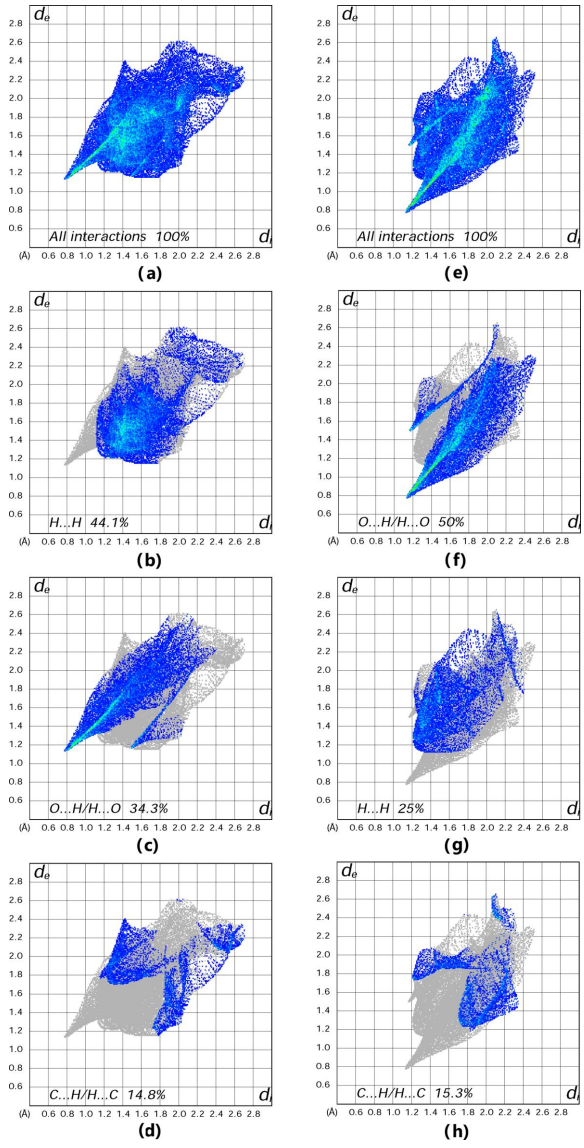

Figure 6
Two-dimensional fingerprint plots for the $[Ni(OPD)_2(H_2O)_2]^{2+}$ cation [parts (*a*), (*b*), (*c*) and (*d*)] and the NDS^{2-}dianion [parts (*e*), (*f*), (*g*) and (*h*)]. The d_i and d_e values are the closest internal and external distances (in Å) from a given point on the Hirshfeld surface.

coordinates to a transition-metal cation (copper) in a monodentate manner (XABPEW; Chen *et al.*, 2002).

5. Synthesis and crystallization

The starting materials are commercially available and were used without further purification. The ligand OPDA (0.216 g, 2 mmol) was dissolved in 10 ml of a 1:1 *v*/*v* ethanol/water mixture. This solution was then added to a solution containing nickel(II) sulfate heptahydrate (0.281 g, 1 mmol) and disodium naphthalene-1,5-disulfonate (0.332 g, 1 mmol) in 10 ml of the same mixed ethanol/water solvent. The resulting mixture was heated under reflux and stirred for 40 min. After 5 d of slow solvent evaporation at room temperature, a light-green crystalline product was obtained with a yield of 65% (based on Ni). Elemental analysis calculated (%) for $C_{22}H_{26}N_4NiO_8S_2$: C 44.24, H 4.39, N 9.38; found: C 44.18, H 4.34, N 9.31.

Table 2
Experimental details.

Crystal data	
Chemical formula	$[Ni(C_6H_8N_2)_2(H_2O)_2](C_{10}H_6O_6S_2)$
M_r	597.30
Crystal system, space group	Monoclinic, $P2_1/n$
Temperature (K)	563
a, b, c (Å)	12.7613 (3), 7.7054 (1), 13.4641 (3)
β (°)	111.554 (2)
V (Å^3)	1231.36 (5)
Z	2
Radiation type	Cu $K\alpha$
μ (mm^{-1})	3.22
Crystal size (mm)	0.22 × 0.18 × 0.14
Data collection	
Diffractometer	XtaLAB Synergy, Single source at home/near, HyPix3000
Absorption correction	Multi-scan (*CrysAlis PRO*; Rigaku OD, 2023)
T_{min}, T_{max}	0.573, 1.000
No. of measured, independent and observed [$I > 2\sigma(I)$] reflections	11384, 2380, 2152
R_{int}	0.038
$(\sin\theta/\lambda)_{max}$ (Å^{-1})	0.614
Refinement	
$R[F^2 > 2\sigma(F^2)]$, $wR(F^2)$, S	0.036, 0.097, 1.04
No. of reflections	2380
No. of parameters	194
No. of restraints	6
H-atom treatment	H atoms treated by a mixture of independent and constrained refinement
$\Delta\rho_{max}$, $\Delta\rho_{min}$ (e Å^{-3})	0.50, −0.49

Computer programs: *CrysAlis PRO* (Rigaku OD, 2023), *SHELXT* (Sheldrick, 2015*a*), *SHELXL* (Sheldrick, 2015*b*), *OLEX2* (Dolomanov *et al.*, 2009).

6. Refinement

Crystal data, data collection and structure refinement details are summarized in Table 2. C-bound H atoms were placed in calculated positions and refined using a riding-model approximation, with $U_{iso}(H) = 1.2U_{eq}(C)$ and C—H = 0.93 Å for aromatic H atoms. Hydrogen atoms of the amino groups and of the water molecule were located using a difference-Fourier map and refined with bond-length restraints of 0.89 (1) and 0.85 (1) Å, respectively.

Funding information

The authors thank the Uzbekistan government for direct financial support of this research. A Grant for Fundamental Research from the Center of Science and Technology of Uzbekistan is gratefully acknowledged.

References

Abdullah, Kh., Hussien, N., Salam, A., Kareem, A., Rahman, A. & Mourad, S. (2019). *Biochem. Cell. Arch.* **19**, 1705–1711.

Adhikari, S., Bhattacharjee, T., Bhattacharjee, S., Daniliuc, C. G., Frontera, A., Lopato, E. M. & Bernhard, S. (2021). *Dalton Trans.* **50**, 5632–5643.
Aniket, P., Shantanu, D. S., Anagha, O. B. & Ajinkya, P. S. (2015). *Int. J. ChemTech Res.* **8**, 496–500.
Bottari, F., Moro, G., Sleegers, N., Florea, A., Cowen, T., Piletsky, S., van Nuijs, A. L. N. & De Wael, K. (2020). *Electroanalysis*, **32**, 135–141.
Chakraborty, P., Jana, A. & Mohanta, S. (2014). *Polyhedron*, **77**, 39–46.
Chen, B., Ye, W., Li, Z., Jin, S., Wang, J., Guo, M. & Wang, D. (2022). *J. Mol. Struct.* **1249**, 131602.
Chen, C. H., Cai, J. W., Feng, X. L. & Chen, X. M. (2002). *Chin. J. Inorg. Chem.* **18**, 659–664.
Chen, J., Li, J., Fu, X., Xie, Q., Zeng, T., Jin, S., Xu, W. & Wang, D. (2020). *J. Mol. Struct.* **1204**, 127491.
Das, D., Mahata, G., Adhikary, A., Konar, S. & Biradha, K. (2015). *Cryst. Growth Des.* **15**, 4132–4141.
Deng, Z.-P., Huo, L.-H., Zhao, H. & Gao, S. (2012). *Cryst. Growth Des.* **12**, 3342–3355.
Djebli, Y., Boufas, S., Bencharif, L., Roisnel, T. & Bencharif, M. (2012). *Acta Cryst.* E**68**, m1411–m1412.
Dolomanov, O. V., Bourhis, L. J., Gildea, R. J., Howard, J. A. K. & Puschmann, H. (2009). *J. Appl. Cryst.* **42**, 339–341.
González Guillén, A., Oszajca, M., Luberda-Durnaś, K., Gryl, M., Bartkiewicz, S., Miniewicz, A. & Lasocha, W. (2018). *Cryst. Growth Des.* **18**, 5029–5037.
Groom, C. R., Bruno, I. J., Lightfoot, M. P. & Ward, S. C. (2016). *Acta Cryst.* B**72**, 171–179.
Huo, L.-H., Gao, S., Xu, S.-X. & Zhao, H. (2005). *Acta Cryst.* E**61**, m449–m450.
Jadoun, S., Riaz, U., Yáñez, J. & Pal Singh Chauhan, N. (2021). *Eur. Polym. J.* **156**, 110600.
Kokunov, Yu. V., Kovalev, V. V., Gorbunova, Yu. E. & Kozyukhin, S. A. (2015). *Russ. J. Inorg. Chem.* **60**, 151–156.
Konieczny, P., González-Guillén, A. B., Luberda-Durnaś, K., Čižmár, E., Pełka, R., Oszajca, M. & Łasocha, W. (2019). *Dalton Trans.* **48**, 7560–7570.
Koroteev, P. S., Ilyukhin, A. B., Babeshkin, K. A. & Efimov, N. N. (2020). *J. Mol. Struct.* **1207**, 127800.
Lian, Z. & Qu, J. (2013). *Z. Kristallogr. New Cryst. Struct.* **228**, 482–484.
Lu, X., Wang, Z. & Liu, M. (2009). *Chin. J. Chem.* **27**, 221–226.
Ngopoh, F. A. I., Lachkar, M., Đorđević, T., Lengauer, C. L. & El Bali, B. (2015). *J. Chem. Crystallogr.* **45**, 369–375.
Oh, H., Kim, D., Kim, D., Park, I.-H. & Jung, O.-S. (2020). *Cryst. Growth Des.* **20**, 7027–7033.
Pardeshi, S. D. & Thore, S. N. (2015). *Int. J. Chem. Phys.* **4**, 300–307.
Pisarevskaya, E. Y., Kolesnichenko, I. I., Averin, A. A., Gorbunov, A. M. & Efimov, O. N. (2020). *Synth. Met.* **270**, 116596.
Rigaku OD (2023). *CrysAlis PRO*. Rigaku Oxford Diffraction Ltd, Yarnton, Oxfordshire, England.
Sabbani, S. & Das, S. K. (2009). *Inorg. Chem. Commun.* **12**, 364–367.
Sagasser, J., Ma, B. N., Baecker, D., Salcher, S., Hermann, M., Lamprecht, J., Angerer, S., Obexer, P., Kircher, B. & Gust, R. (2019). *J. Med. Chem.* **62**, 8053–8061.
Sayyah, S. M., El–Deeb, M. M., Kamal, S. M. & Azooz, R. (2009). *J. Appl. Polym. Sci.* **112**, 3695–3706.
Sheldrick, G. M. (2015*a*). *Acta Cryst.* A**71**, 3–8.
Sheldrick, G. M. (2015*b*). *Acta Cryst.* C**71**, 3–8.
Shi, Ch., Wei, B. & Zhang, W. (2014). *Cryst. Growth Des.* **14**, 6570–6580.
Spackman, P. R., Turner, M. J., McKinnon, J. J., Wolff, S. K., Grimwood, D. J., Jayatilaka, D. & Spackman, M. A. (2021). *J. Appl. Cryst.* **54**, 1006–1011.
Tai, X.-S., Zhang, Y.-P. & Zhao, W.-H. (2015). *Res. Chem. Intermed.* **41**, 4339–4347.
Vishvanath, D. P. & Ketan, P. P. (2014). *Int. J. ChemTech Res.* **8**, 457–465.
Willett, R. D., Gómez-García, C. J., Twamley, B., Gómez-Coca, S. & Ruiz, E. (2012). *Inorg. Chem.* **51**, 5487–5493.
Xu, W., Lu, Y., Xia, Y. Y., Liu, B., Jin, S., Zhong, B., Wang, D. & Guo, M. (2019). *J. Mol. Struct.* **1189**, 81–93.
Zick, P. L. & Geiger, D. K. (2016). *Acta Cryst.* E**72**, 1037–1042.

supporting information

Acta Cryst. (2023). E**79**, 1083-1087 [https://doi.org/10.1107/S2056989023009350]

Synthesis, crystal structure and Hirshfeld surface analysis of diaquabis(*o*-phenylenediamine-κ^2N,N')nickel(II) naphthalene-1,5-disulfonate

Jabbor R Suyunov, Khayit Kh. Turaev, Bekmurod Kh. Alimnazarov, Yusuf E. Nazarov, Islombek J. Mengnorov, Bakhtiyar T. Ibragimov and Jamshid M. Ashurov

Computing details

Data collection: *CrysAlis PRO* (Rigaku OD, 2023); cell refinement: *CrysAlis PRO* (Rigaku OD, 2023); data reduction: *CrysAlis PRO* (Rigaku OD, 2023); program(s) used to solve structure: *SHELXT* (Sheldrick, 2015a); program(s) used to refine structure: *SHELXL* (Sheldrick, 2015b); molecular graphics: Olex2 (Dolomanov *et al.*, 2009); software used to prepare material for publication: Olex2 (Dolomanov *et al.*, 2009).

Diaquabis(*o*-phenylenediamine-κ^2N,N')nickel(II) naphthalene-1,5-disulfonate

Crystal data

$[Ni(C_6H_8N_2)_2(H_2O)_2](C_{10}H_6O_6S_2)$
M_r = 597.30
Monoclinic, $P2_1/n$
a = 12.7613 (3) Å
b = 7.7054 (1) Å
c = 13.4641 (3) Å
β = 111.554 (2)°
V = 1231.36 (5) Å^3
Z = 2
$F(000)$ = 620
D_x = 1.611 Mg m^{-3}
Cu $K\alpha$ radiation, λ = 1.54184 Å
Cell parameters from 6737 reflections
θ = 4.1–71.0°
μ = 3.22 mm^{-1}
T = 563 K
Block, light green
0.22 × 0.18 × 0.14 mm

Data collection

XtaLAB Synergy, Single source at home/near, HyPix3000 diffractometer
Radiation source: micro-focus sealed X-ray tube, PhotonJet (Cu) X-ray Source
Mirror monochromator
Detector resolution: 10.0000 pixels mm^{-1}
ω scans
Absorption correction: multi-scan (CrysAlisPro; Rigaku OD, 2023)
T_{min} = 0.573, T_{max} = 1.000
11384 measured reflections
2380 independent reflections
2152 reflections with $I > 2\sigma(I)$
R_{int} = 0.038
θ_{max} = 71.3°, θ_{min} = 4.1°
h = −15→15
k = −9→9
l = −14→16

Refinement

Refinement on F^2
Least-squares matrix: full
$R[F^2 > 2\sigma(F^2)]$ = 0.036
$wR(F^2)$ = 0.097
S = 1.04
2380 reflections
194 parameters
6 restraints
Primary atom site location: iterative
Hydrogen site location: mixed
H atoms treated by a mixture of independent and constrained refinement

$w = 1/[\sigma^2(F_o^2) + (0.048P)^2 + 0.8302P]$
where $P = (F_o^2 + 2F_c^2)/3$
$(\Delta/\sigma)_{max} = 0.001$
$\Delta\rho_{max} = 0.50$ e Å^{-3}
$\Delta\rho_{min} = -0.49$ e Å^{-3}
Extinction correction: SHELXL (Sheldrick, 2015a), $Fc^* = kFc[1+0.001xFc^2\lambda^3/\sin(2\theta)]^{-1/4}$
Extinction coefficient: 0.0006 (2)

Special details

Geometry. All esds (except the esd in the dihedral angle between two l.s. planes) are estimated using the full covariance matrix. The cell esds are taken into account individually in the estimation of esds in distances, angles and torsion angles; correlations between esds in cell parameters are only used when they are defined by crystal symmetry. An approximate (isotropic) treatment of cell esds is used for estimating esds involving l.s. planes.

Fractional atomic coordinates and isotropic or equivalent isotropic displacement parameters (Å^2)

	x	*y*	*z*	U_{iso}*/U_{eq}
Ni1	1.000000	0.500000	0.500000	0.02713 (17)
S1	0.69836 (5)	0.87424 (8)	0.39745 (4)	0.03779 (18)
O1W	0.83329 (14)	0.4677 (2)	0.38469 (14)	0.0412 (4)
O1	0.73435 (15)	0.7254 (2)	0.46852 (14)	0.0488 (5)
N1	0.99045 (16)	0.2387 (2)	0.53808 (16)	0.0330 (4)
O3	0.62288 (17)	0.8217 (3)	0.29283 (14)	0.0574 (5)
N2	0.93181 (15)	0.5408 (2)	0.61643 (14)	0.0298 (4)
O2	0.79217 (17)	0.9758 (3)	0.39332 (19)	0.0636 (6)
C11	0.47191 (16)	1.0579 (3)	0.52339 (16)	0.0276 (4)
C6	0.91414 (17)	0.3765 (3)	0.66003 (16)	0.0297 (4)
C1	0.94563 (18)	0.2253 (3)	0.62287 (17)	0.0319 (5)
C7	0.62041 (18)	1.0098 (3)	0.45202 (17)	0.0313 (5)
C10	0.50918 (19)	1.2316 (3)	0.54324 (18)	0.0350 (5)
H10	0.473811	1.306841	0.575033	0.042*
C5	0.86718 (19)	0.3671 (3)	0.73833 (18)	0.0381 (5)
H5	0.846130	0.468202	0.763862	0.046*
C8	0.65220 (18)	1.1796 (3)	0.47028 (19)	0.0385 (5)
H8	0.711068	1.221455	0.451995	0.046*
C9	0.5960 (2)	1.2909 (3)	0.5166 (2)	0.0405 (5)
H9	0.618250	1.406318	0.529312	0.049*
C2	0.9316 (2)	0.0661 (3)	0.6643 (2)	0.0446 (6)
H2	0.953980	−0.035050	0.639981	0.054*
C4	0.8518 (2)	0.2078 (4)	0.7781 (2)	0.0474 (6)
H4	0.819333	0.201834	0.829604	0.057*
C3	0.8845 (2)	0.0572 (4)	0.7417 (2)	0.0510 (6)
H3	0.874888	−0.049782	0.769179	0.061*
H2A	0.8674 (14)	0.596 (3)	0.585 (2)	0.049 (8)*
H2B	0.9775 (17)	0.607 (3)	0.6689 (15)	0.038 (7)*
H1A	0.946 (2)	0.188 (4)	0.4786 (15)	0.062 (9)*
H1B	1.0556 (14)	0.182 (3)	0.561 (2)	0.052 (8)*
H1WA	0.822 (3)	0.447 (5)	0.3199 (11)	0.072 (11)*
H1WB	0.787 (2)	0.546 (4)	0.386 (3)	0.085 (12)*

Atomic displacement parameters (Å²)

	U^{11}	U^{22}	U^{33}	U^{12}	U^{13}	U^{23}
Ni1	0.0287 (3)	0.0260 (3)	0.0306 (3)	0.00340 (18)	0.0155 (2)	0.00141 (19)
S1	0.0365 (3)	0.0456 (3)	0.0367 (3)	0.0168 (2)	0.0198 (2)	0.0050 (2)
O1W	0.0343 (9)	0.0495 (10)	0.0395 (9)	0.0062 (7)	0.0133 (7)	−0.0073 (8)
O1	0.0481 (10)	0.0549 (11)	0.0464 (10)	0.0299 (8)	0.0208 (8)	0.0131 (8)
N1	0.0353 (10)	0.0280 (9)	0.0418 (11)	0.0046 (8)	0.0212 (9)	0.0015 (8)
O3	0.0633 (12)	0.0736 (14)	0.0348 (9)	0.0262 (10)	0.0175 (9)	−0.0035 (9)
N2	0.0291 (9)	0.0302 (9)	0.0316 (9)	0.0041 (7)	0.0131 (8)	−0.0002 (7)
O2	0.0550 (12)	0.0644 (13)	0.0938 (17)	0.0090 (10)	0.0538 (12)	0.0030 (11)
C11	0.0259 (9)	0.0302 (10)	0.0258 (9)	0.0070 (8)	0.0085 (8)	0.0004 (8)
C6	0.0246 (10)	0.0356 (11)	0.0280 (10)	0.0001 (8)	0.0088 (8)	0.0024 (8)
C1	0.0294 (10)	0.0331 (11)	0.0347 (11)	0.0014 (8)	0.0135 (9)	0.0040 (9)
C7	0.0279 (10)	0.0368 (11)	0.0300 (10)	0.0089 (8)	0.0117 (9)	0.0014 (8)
C10	0.0348 (11)	0.0331 (11)	0.0374 (11)	0.0067 (9)	0.0137 (9)	−0.0044 (9)
C5	0.0349 (11)	0.0492 (14)	0.0331 (11)	−0.0016 (10)	0.0158 (9)	−0.0019 (10)
C8	0.0286 (11)	0.0411 (12)	0.0475 (13)	0.0015 (9)	0.0160 (10)	0.0034 (10)
C9	0.0386 (12)	0.0301 (11)	0.0516 (14)	−0.0005 (9)	0.0153 (11)	−0.0049 (10)
C2	0.0493 (14)	0.0354 (12)	0.0517 (15)	0.0012 (11)	0.0217 (12)	0.0085 (11)
C4	0.0461 (14)	0.0645 (17)	0.0366 (12)	−0.0081 (12)	0.0209 (11)	0.0059 (12)
C3	0.0573 (16)	0.0501 (15)	0.0487 (15)	−0.0050 (13)	0.0231 (13)	0.0153 (12)

Geometric parameters (Å, º)

Ni1—O1W^{i}	2.1381 (17)	C11—C7^{ii}	1.434 (3)
Ni1—O1W	2.1381 (17)	C11—C10	1.413 (3)
Ni1—N1	2.0924 (18)	C6—C1	1.385 (3)
Ni1—N1^{i}	2.0924 (18)	C6—C5	1.393 (3)
Ni1—N2^{i}	2.0776 (17)	C1—C2	1.386 (3)
Ni1—N2	2.0775 (17)	C7—C8	1.365 (3)
S1—O1	1.4558 (18)	C10—H10	0.9300
S1—O3	1.4419 (19)	C10—C9	1.363 (3)
S1—O2	1.448 (2)	C5—H5	0.9300
S1—C7	1.777 (2)	C5—C4	1.382 (4)
O1W—H1WA	0.846 (10)	C8—H8	0.9300
O1W—H1WB	0.850 (10)	C8—C9	1.403 (3)
N1—C1	1.456 (3)	C9—H9	0.9300
N1—H1A	0.886 (10)	C2—H2	0.9300
N1—H1B	0.889 (10)	C2—C3	1.383 (4)
N2—C6	1.447 (3)	C4—H4	0.9300
N2—H2A	0.882 (10)	C4—C3	1.383 (4)
N2—H2B	0.891 (10)	C3—H3	0.9300
C11—C11^{ii}	1.427 (4)		
O1W—Ni1—O1W^{i}	180.0	H2A—N2—H2B	109 (3)
N1^{i}—Ni1—O1W^{i}	86.20 (8)	C11^{ii}—C11—C7^{ii}	117.6 (2)
N1^{i}—Ni1—O1W	93.80 (8)	C10—C11—C11^{ii}	119.1 (2)

N1—Ni1—O1W^{i}	93.80 (8)	C10—C11—C7^{ii}	123.28 (19)
N1—Ni1—O1W	86.20 (8)	C1—C6—N2	118.72 (18)
N1—Ni1—N1^{i}	180.0	C1—C6—C5	119.5 (2)
N2^{i}—Ni1—O1W	90.88 (7)	C5—C6—N2	121.8 (2)
N2^{i}—Ni1—O1W^{i}	89.12 (7)	C6—C1—N1	118.23 (19)
N2—Ni1—O1W	89.12 (7)	C6—C1—C2	120.1 (2)
N2—Ni1—O1W^{i}	90.88 (7)	C2—C1—N1	121.6 (2)
N2^{i}—Ni1—N1^{i}	83.26 (7)	C11^{ii}—C7—S1	120.95 (16)
N2—Ni1—N1^{i}	96.74 (7)	C8—C7—S1	117.60 (17)
N2—Ni1—N1	83.26 (7)	C8—C7—C11^{ii}	121.45 (19)
N2^{i}—Ni1—N1	96.74 (7)	C11—C10—H10	119.4
N2—Ni1—N2^{i}	180.00 (10)	C9—C10—C11	121.2 (2)
O1—S1—C7	106.30 (10)	C9—C10—H10	119.4
O3—S1—O1	110.91 (13)	C6—C5—H5	119.9
O3—S1—O2	112.29 (13)	C4—C5—C6	120.1 (2)
O3—S1—C7	107.13 (10)	C4—C5—H5	119.9
O2—S1—O1	112.67 (12)	C7—C8—H8	120.0
O2—S1—C7	107.12 (11)	C7—C8—C9	120.0 (2)
Ni1—O1W—H1WA	121 (2)	C9—C8—H8	120.0
Ni1—O1W—H1WB	115 (3)	C10—C9—C8	120.7 (2)
H1WA—O1W—H1WB	107 (3)	C10—C9—H9	119.7
Ni1—N1—H1A	106 (2)	C8—C9—H9	119.7
Ni1—N1—H1B	115 (2)	C1—C2—H2	119.9
C1—N1—Ni1	109.60 (13)	C3—C2—C1	120.2 (2)
C1—N1—H1A	112 (2)	C3—C2—H2	119.9
C1—N1—H1B	106.1 (19)	C5—C4—H4	119.9
H1A—N1—H1B	108 (3)	C5—C4—C3	120.2 (2)
Ni1—N2—H2A	107.0 (18)	C3—C4—H4	119.9
Ni1—N2—H2B	110.6 (16)	C2—C3—H3	120.1
C6—N2—Ni1	110.14 (13)	C4—C3—C2	119.8 (2)
C6—N2—H2A	110.8 (19)	C4—C3—H3	120.1
C6—N2—H2B	109.3 (17)		

Ni1—N1—C1—C6	2.3 (2)	O2—S1—C7—C8	5.8 (2)
Ni1—N1—C1—C2	−179.29 (18)	C11^{ii}—C11—C10—C9	1.3 (4)
Ni1—N2—C6—C1	1.6 (2)	C11^{ii}—C7—C8—C9	1.7 (3)
Ni1—N2—C6—C5	−178.80 (17)	C11—C10—C9—C8	−1.1 (4)
S1—C7—C8—C9	−177.84 (18)	C6—C1—C2—C3	1.0 (4)
O1—S1—C7—C11^{ii}	−53.0 (2)	C6—C5—C4—C3	1.0 (4)
O1—S1—C7—C8	126.48 (19)	C1—C6—C5—C4	−0.3 (3)
N1—C1—C2—C3	−177.3 (2)	C1—C2—C3—C4	−0.3 (4)
O3—S1—C7—C11^{ii}	65.6 (2)	C7^{ii}—C11—C10—C9	−178.7 (2)
O3—S1—C7—C8	−114.9 (2)	C7—C8—C9—C10	−0.4 (4)
N2—C6—C1—N1	−2.7 (3)	C5—C6—C1—N1	177.67 (19)
N2—C6—C1—C2	178.9 (2)	C5—C6—C1—C2	−0.8 (3)

N2—C6—C5—C4	−179.9 (2)	C5—C4—C3—C2	−0.7 (4)
O2—S1—C7—C11^{ii}	−173.73 (18)		

Symmetry codes: (i) −*x*+2, −*y*+1, −*z*+1; (ii) −*x*+1, −*y*+2, −*z*+1.

Hydrogen-bond geometry (Å, º)

D—H···*A*	*D*—H	H···*A*	*D*···*A*	*D*—H···*A*
N1—H1*A*···O2^{iii}	0.89 (1)	2.48 (2)	3.268 (3)	148 (3)
N1—H1*B*···O2^{i}	0.89 (1)	2.18 (1)	3.066 (3)	175 (3)
N2—H2*A*···O1	0.88 (1)	2.10 (1)	2.941 (2)	160 (3)
N2—H2*B*···O3^{iv}	0.89 (1)	2.06 (1)	2.908 (3)	158 (2)
O1*W*—H1*WA*···O3^{v}	0.85 (1)	2.12 (2)	2.876 (3)	148 (3)
O1*W*—H1*WB*···O1	0.85 (1)	2.04 (2)	2.803 (2)	150 (3)

Symmetry codes: (i) −*x*+2, −*y*+1, −*z*+1; (iii) *x*, *y*−1, *z*; (iv) *x*+1/2, −*y*+3/2, *z*+1/2; (v) −*x*+3/2, *y*−1/2, −*z*+1/2.